RSC Advances

ROYAL SOCIETY OF CHEMISTRY

www.rsc.org/advances

Journal Name

RSCPublishing

COMMUNICATION

Precise aggregation-induced emission enhancement *via* H^+ sensing and its use in ratiometric detection of intracellular pH values†

Cite this: DOI: 10.1039/x0xx00000x

Received 00th January 2012,
Accepted 00th January 2012

DOI: 10.1039/x0xx00000x

www.rsc.org/

Anushri Rananaware,[a] Rajesh S. Bhosale,[b,c], Hemlata Patil,[a] Mohammad Al Kobaisi,[d] Amanda Abraham[a], Ravi Shukla,[a] Sidhanath V. Bhosale,[b] Sheshanath V. Bhosale[a,*]

A pyridyl functionalised tetraphenylethylene (Py-TPE) for ratiometric fluorescent detection of intracellular pH values has been reported. The Py-TPE fluorescent probe can be used for H^+ sensing in organic solvents ($CHCl_3$, DMF and MeOH) and the change in optical density through absorption, emission and naked eye detection was modulated. On addition of TFA, an aggregation-induced enhancement of emission with increase in quantum yield of 0.11 to 0.63, due to intramolecular charge transfer (ICT) process. This process is reversed by addition of TEA resulting in a cycle that can be repeated several times.

Recent years, the development of mechanochromic luminescent materials has gained much attention due to their potential applicability in the various fields such as mechano-sensors, security papers, and optoelectronic devices.[1] The key requirement for mechanochromic luminescent materials are the solid state emission and high contrast.[2] On the other hand, the conventional fluorescent aromatic molecules suffer from aggregation caused quenching (ACQ) in solid state emission.[3] To overcome ACQ issues, earlier Tang group, introduced a novel concept, which is called aggregation induced emission (AIE).[4] Later Park and co-workers introduced aggregation-induced enhanced emission (AIEE).[5] AIE and AIEE molecules shown to be highly fluorescent in the solid state, which is an essential requirement for mechanochromism. Thereafter, tetrapheneylethene (TPE) molecule were introduced and shown very interesting properties, as they are non-emissive in the dissolved state but enhanced emission could be seen in both the aggregated form and the solid state.[6] Taking advantage of this phenomenon, a number of groups have functionalised TPE for various applications such as chemosensors, bio-probes, and solid-state emitters, and real-time cell apoptosis imaging.[7,8] Interestingly, it has also been used for fluorescence ''turn on'' chemosensors for selective detection of Ag^+ and Hg^{2+} ions.[9]

In earlier work, tetrapyridyl-substituted tetraphenylethylenes have been reported for various application such as supramolecular building blocks,[10] TPE-based organic and metal–organic networks,[11] mercury sensing,[12] and halogen bonded network[13]. We are interested to use pyridyl functionalised dyes as a pH sensor as well as study their acid induced assembly.[14] In this work, we report the pyridyl appended TPE motif **1** (Figure 1) and its dual applications: firstly its use as a reversible probe for acid/base sensing in solution and live cells, and secondly, the pH- and solvent-dependent assembly. The protonation/deprotonation can be detected by naked eye, as color of the solution changed from light yellow to dark green (λ_{ex} = 365 nm) in acidic condition by addition of trifluoroacetic acid (TFA) and reversed to light yellow upon addition of triethylamine (TEA) in various solvents such as chloroform ($CHCl_3$), *N,N'*-Dimethylformamide (DMF) and methanol (MeOH) as shown in Figure 1b. The fluorescence intensity is enhanced more efficiently in chloroform in comparison to DMF and MeOH. This is because ionic species can aggregate to a higher extent in a nonprotic solvent such as $CHCl_3$, while DMF and MeOH are able to solvate protonated Py-TPE ionic species resulting in less aggregation and therefore less AIE. Furthermore, spectroscopic and scanning electron microscopic (SEM) techniques were employed to demonstrate the growth mechanism.

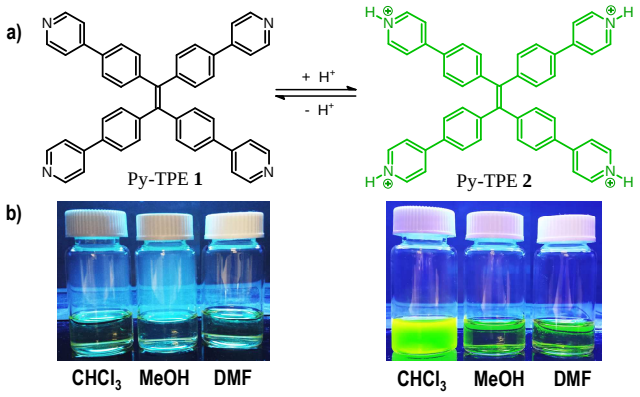

Fig. 1 (a) Illustration of protonation/deprotonation of Py-TPE molecules (**1** and **2**) and (b) Shows florescent images, taken under UV light (λ_{ex} = 365 nm) for the solution containing Py-TPE **1** or **2** (0.5 μM) with and without TFA (2 μM) in respective solvents under illumination at 298 K.

Pyridyl substituted TPE **1** (Py-TPE **1**) was prepared *via* Suzuki coupling reaction of tetrabromo TPE with 4-pyridine boronic acid in the presence of $Pd(PPh_3)_4$ as reported in literature.[10] Py-TPE **1** bears two important features, allowing molecules to self-assemble into a variety of supramolecular nanostructures with pH control, the first is the pyridyl moiety for protonation, which may tune the intermolecular interaction by charge pairing, and the second is the planar aromatic core of TPE for packing the structures *via* π–π-interactions and Van der Walls forces.

Py-TPE **1** can be dissolved easily in organic solvents such as $CHCl_3$, DMF and MeOH, resulting in a stable, transparent light yellow solution. In $CHCl_3$, **1** (1×10^{-5} M) showed two well-resolved absorption bands at 276 nm, and 310 nm, assigned to the $S_0\rightarrow S_2$, and the $S_0\rightarrow S_1$ transitions respectively, and a shoulder at 339 nm, which is typical of the TPE chromophore (Fig. 2a). Almost identical UV-vis absorption was observed in DMF and MeOH. Interestingly, upon addition of TFA in $CHCl_3$ a significant increase at 342 nm bands was observed along with decrease of both 276 nm and 310 nm bands, in DMF and MeOH, the 342 nm band appeared red-shifted to 351 nm. Figure 2b illustrates the typical absorption of **1** in $CHCl_3$ with the gradual addition of 0-10 equiv. TFA (10^{-4} M), a slight red shift of the absorption maxima to 342 nm with gradual increase in its intensity is observed. These results clearly indicate that such a shift in the absorption is due to protonation of pyridine group along with charge-pairing and hydrogen-bonding, in addition to dipole–dipole interactions relative to the $S_0\rightarrow S_1$ transition. Py-TPE-H^+ (**2**) can be deprotonated by the addition of a TEA to regenerate Py-TPE **1** and this reverse cycle is seen in all the organic solvents used in this study (see Supporting Information Fig. S1a-c).

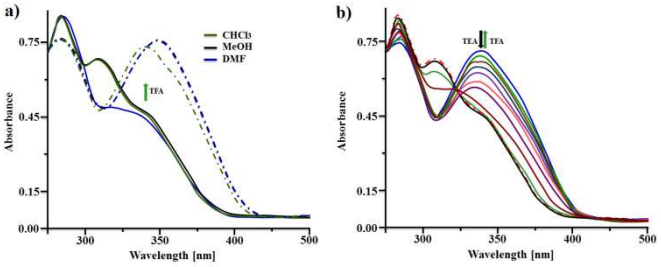

Fig. 2 UV-vis absorption spectral changes of Py-TPE **1** (1×10^{-5} M): (a) with and without addition of TFA (10^{-2} M) in $CHCl_3$, MeOH and DMF, respectively, and (b) upon gradual addition of TFA (10^{-4} M, 0-20 equiv.) in $CHCl_3$.

Furthermore, we study protonation/deprotonation cycle using fluorescence microscopy. We found that, Py-TPE **1** is weakly florescent (λ_{em} = ~480 nm, λ_{ex} = 340 nm) in the organic solvents such as $CHCl_3$, DMF and MeOH, and even gradual addition of water (up to 70%) in the later two solvents had very little effect on the fluorescence spectra of **1** which is markedly fluorescent in the solid state i.e. band appeared at 438 and 562 nm and in water at 425 and 550 nm, however upon protonation of Pt-TPE **1** emission bands broaden with red shift to 440 and 540 nm, respectively (see supporting information Fig. S3 & S4). In $CHCl_3$ an emission maximum at 440 nm was observed and in DMF and MeOH, the band had a similar shape to that in $CHCl_3$, but was red-shifted to 448 nm. Interestingly, upon addition of trifluoroacetic acid (TFA) the emission was significantly enhanced and red shifted to ~534 nm, this fluorescence enhancement was observed only in $CHCl_3$, DMF and MeOH (See Supporting Information Fig. S2). This process is reversible upon addition of triethylamine (TEA) to the solution of **1** in DMF, restoring fluorescence to its original state (Fig. 3a). In acidic condition, emission intensity increased, with about 86 nm red shift of the emission to 534 nm with an isosbestic point at 472 nm. In DMF, acidification caused the intensity of the fluorescence to increase (Φ = ~0.73) and after the addition of TEA, the original fluorescence (Φ = 0.18) spectrum of **1** was obtained; this cycle is reversed several times without any loss of emission intensity (Fig. 3b).[15,16] This phenomenon was observed in all the organic solvents used in this study (see Supporting Information Fig. S2a-c). Thus, the fluorescence spectra showed clear bathochromic shifts and enhancement of emission in the case of **2** over the non-protonated species **1** can be attributed to an intramolecular charge transfer (ICT) process and π–π–stacking of the aromatic cores in polar solvent. Similar phenomenon was reported in the case of 3-acetyl-6-(4-vinylpyridine)-9-ethyl- carbazole by Yu and co-workers.[17] ^{1}H-NMR spectroscopy conforms the protonation of **1** resulting in a downfield shifts of the aromatic peaks of the pyridine moieties i.e. from δ = 7.5 to 7.63 ppm and from d = 8.62 to 8.69 ppm (See Supporting Information Fig. S5).

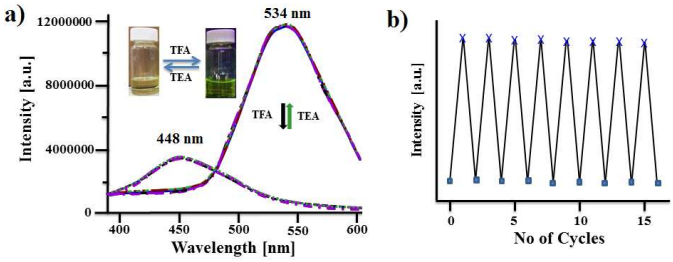

Fig. 3 (a) Fluorescence emission spectra of **1** (1×10^{-5} M) in DMF solution with alternating addition of TFA and TEA (λ_{ex} = 365 nm). (b) Fluorescence intensity vs. number of additions of TFA and TEA at 534 nm. It is important to mention here that the absorption of **2** at 340 nm is approximately twice higher than that of **1** in DMF.

Theoretical density functional theory (DFT) calculations using Gaussian 09 suite of programs[18] and B3LYP/6-31G level of theory of the unprotonated Py-TPE **(1)** and quadrople protonated Py-TPE **(2)** molecules indicated that HOMO→LUMO transition red shifts by 67.265 nm when protonated, this is consistent with the UV-Vis and spectroscopy evidence in solution (See Supporting Information Fig. S6-S8 and Table S1). Calculation also show positive charge distributed across the molecule through the conjugated aromatic system in **(2)**, this makes π-π - stacking of solubilised **(1)** in aqueous acidic media less likely and hence the disappearance of AIE effect, ion paring is dominant interaction in organic solvents.

Time-dependent density functional theory (TD-DFT) and B3LYP/6-31G level of theory is applied to the electronic excited states of **1** and **2**. The calculation is performed for both singlet and triplet of 4 excited states in gas phase. Py-TPE **2**, shows a redshift in the obtained transition and also the fluorescence peak in the visible region can be assigned to a triplet ^{3}A transition with oscillator strength f = 0 making the irradiative process less likely. Thus, the aggregation of the protonated or unprotonated species causes the

rotation in the arms of the molecule which is found to play important role in dissipating excited state energy to be hindered.[19] This makes the radiate decay to be enhanced at room temperature. Similar phenomenon was observed in solid state.

To gain further insight, we investigated Scanning Electron Microscopy (SEM). Self-assembled aggregation arrangement of the protonated pyridyl functionalised tetraphenylethylene molecules **2** (10^{-5} M) forms needle shaped crystals in a fractal pattern (Fig. 4) with various dimensions was determined by SEM.

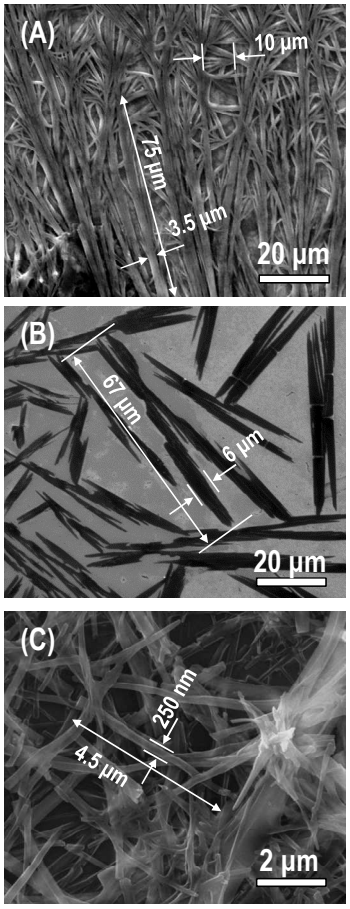

Fig. 4 Scanning electron micrographs of **2** (10^{-5} M) recrystallized from (A) DMF, (B) MeOH and (C) $CHCl_3$.

Typically, larger crystallites were observed to form DMF (A) and smaller were formed by MeOH (B) and $CHCl_3$ (C) after solvent evaporation. However, crystal formation seems to be less frequently from polar solvent such as DMF and MeOH. And, the width of crystals varies depending on solvent polarity such as in DMF it is about 3.5 µm, in MeOH ~6 µm, and about 250 nm in $CHCl_3$. Many cross-linked nanostructures were also observed from these solvents, but no precipitation or collapsed morphology was apparent. These results suggesting that the formed crystalline aggregates are very stable. As expected the formed aggregates disappeared upon the addition of TEA. Even increasing concentration of **2** (10^{-3} M) in all above solvents does not change any aggregation morphology, only extended aggregates was observed (See Supporting Fig. S9). On the other hand, unprotonated form of Py-TPE **1** in MeOH and DMF aggregates into non-crystalline global supramolecular aggregates (See Supporting Information Fig. S10A and S10B), which may be due to a phase transition from monomer into aggregates in the polar solvents. In contrast, compound **1**, form large circles in $CHCl_3$ after evaporation on surface (Fig. S8C). In unprotonated form soluble species and the disappearance of AIEE of the Py-TPE was observed, a similar effect has been observed in the case of J- and H-type of aggregates of perylene diimides.[20] Upon protonation and the formation of nano-aggregates *via* self-assembly and enhance the fluorescence emission.[21] This highlights delicate balance of the protonation to tune the ICT effect along with intermolecular interactions (charge pairing and hydrogen bonding) as well as dipole–dipole interactions, allowing nanostructures to form in a controlled fashion.

The potential utility of Py-TPE **1** for the specific imaging of acid-base sensing in living cells was evaluated (Fig. 5). For this purpose **1** was solubilised in DMSO at a 0.5mg/mL stock concentration that was further diluted in serum containing media without any precipitation. Human prostate cancer (PC-3) cells, in their log phase of growth, were cultured in 24 well tissue culture plates for a period of 24 h.

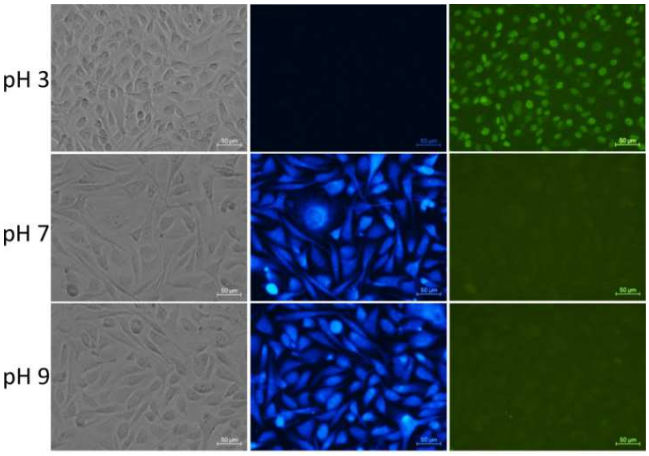

Fig. 5 Fluorescence microscopic images of PC-3 cells treated with 5µg/ml of **1** for two hours at different pH conditions. At lower pH cells show fluorescence in the green channel while at pH higher the 7 cells show fluorescence in blue channel. However no fluorescence was observed in the red channel. Control untreated cells did not show any fluoresces. In the left panel bright field phase contrast images are shown for the same field of view. The size bars in figure correspond to 50µM.

The cells were pre-treated with 5µg/mL of **1** for 2 hours and washed extensively with ice cold PBS to remove any trace amount of unreacted Py-TPE **1**. This leads to significantly low ionic transport through channel proteins and helps in maintenance of cellular architecture. This is clearly reflected from figure 5 where in cells are able to maintain their shape and integral membrane structure. Fluorescence of the cells was observed at lower temperature under acidic (pH 3), neutral (pH 7) and alkaline (pH 9) environments. The lower temperature helps in maintenance of cell integrity under extreme pH conditions across cell membrane as the activity of channel proteins, responsible for movement of ions across the membrane, is significantly hindered due to reduced metabolic activities. Hence, the cells can withstand greater disparity in the

ionic concentration across the membrane. Our fluorescence microscopy images as shown in figure 5 revealed that cells showed a bright fluorescence in the blue channel between 450 and 490 nanometers with a centre wavelength of 470 nanometres at neutral pH condition, and by increasing pH up to 9, the fluorescence remained unaltered. However, when the cells were exposed to acidic conditions a significant red shift in the overall florescence was observed in the green visible light region, in the range between 520 and 560 nanometers. The morphology of cells in phase contrast images on the left side panel of Figure 5 clearly suggests that a 5µg/mL concentration of **1** was nontoxic to cells from. The clean background in the pictures suggests that the **1** is specific to cells and provided significant imaging contrast at the concentrations as low as 5µg/mL.

In summary, we have demonstrated that a pyridyl-substituted tetraphenyleneethylene undergoes protonation and deprotonation event in polar and non-polar solvents. The protonation effect has been studied by means of UV-vis, fluorescence, ^{1}H NMR spectroscopy. The protonation/deprotonation of Py-TPE **1** results in aggregation in acidic condition and hence aggregation-induced enhanced emission (AIEE) effect can be detected by naked eye, and is fully reversible when conditions are oscillating between acidic and basic. The adequate aqueous solubility and appreciable biocompatibility at imaginable concentrations make this compound promising for cell based imaging and sensing applications. Furthermore, protonated species aggregates in organic solvents into a variety of nanostructures depending on solvent used. These results shift in absorption and enhancement in fluorescence attribute to the formation of nano-aggregated assemblies caused due to ICT effect along with π–π-staking becomes dominant and AIEE in protonates form of the Py-TPE. In unprotonated form soluble species and the disappearance of AIEE of the Py-TPE was observed. This colorimetric and ratiometric probe may find promising applications as an active element of chemo- and biosensors.

Acknowledgements

This work was financially support by the Australian Research Council under a Future Fellowship Scheme (FT110100152) and RMIT Microscopy and Microanalysis Facility (RMMF). S. V. B. (IICT) is grateful for financial support from the DAE-BRNS (Project Code: 37(2)/14/08/2014-BRNS), Mumbai.

Notes and references

[a] *School of Applied Sciences, RMIT University, GPO Box 2476, Melbourne, VIC-3001, Australia, E-mail: sheshanath.bhosale@rmit.edu.au*

[b] *Polymers and Functional Materials Division, CSIR-Indian Institute of Chemical Technology, Hyderabad-500 007,Telangana, India*

[c] *RMIT-IICT Research Centre, CSIR-Indian Institute of Chemical Technology, Hyderabad-500 007,Telangana, India*

[d] *Faculty of Science, Engineering and Technology, Swinburne University, PO BOX 3122, Hawthron, Australia*

† Electronic Supplementary Information (ESI) available: Details of UV/vis fluorescence and microscopic data of aggregates in all the solvents. See DOI: 10.1039/c000000x/

1 Y. Sagara and T. Kato, *Nat. Chem.*, 2009, **1**, 605; D. A. Davis, A. Hamilton, J. L. Yang, L. D. Cremar, D. Van Gough, S. L. Potisek, M. T. Ong, P. V. Braun, T. J. Martinez, S. R. White, J. S. Moore and N. R. Sottos, *Nature*, 2009, **459**, 68; Y. J. Dong, B. Xu, J. B. Zhang, X. Tan, L. J. Wang, J. L. Chen, H. G. Lv, S. P. Wen, B. Li, L. Ye, B. Zou and W. J. Tian, *Angew. Chem., Int. Ed*., 2012, **51**, 10782; X. L. Luo, J. N. Li, C. H. Li, L. P. Heng, Y. Q. Dong, Z. P. Liu, Z. S. Bo and B. Z. Tang, *Adv. Mater.*, 2011, **23**, 3261; Q. A. Best, N. Sattenapally, D. J. Dyer, C. N. Scott and M. E. McCarroll, *J. Am. Chem. Soc*., 2013, **135**, 13365.

2. M. S. Kwon, J. Gierschner, S. J. Yoon and S. Y. Park, *Adv. Mater.*, 2012, **24**, 5487.

3 H. J. Tracy, J. L. Mullin, W. T. Klooster, J. A. Martin, J. Haug, S. Wallace, I. Rudloe and K. Watts, *Inorg. Chem.*, 2005, **44**, 2003.

4 J. D. Luo, Z. L. Xie, J. W. Y. Lam, L. Cheng, H. Y. Chen, C. F. Qiu, H. S. Kwok, X. W. Zhan, Y. Q. Liu, D. B. Zhu and B. Z. Tang, *Chem. Commun.*, 2001, 1740.

5 B.-K. An, S.-K. Kwon, S.-D. Jung and S. Y. Park, *J. Am. Chem. Soc.*, 2002, **124**, 14410.

6 H. Tong, Y. Hong, Y. Dong, M. Haüßler, J. W. Y. Lam, Z. Li, Z. Guo, Z. Guo and B. Z. Tang, *Chem. Commun.*, 2006, 3705.

7 Y. Dong, J. W. Y. Lam, A. Qin, J. Liu, Z. Li, B. Z. Tang, J. Sun and H. S. Kwok, *Appl. Phys. Lett.*, 2007, **91**, 11111; H. Tong, Y. Hong, Y. Dong, M. Ha¨ussler, Z. Li, J. W. Y. Lam, Y. Dong, H. H. Y. Sung, I. D. Williams and B. Z. Tang, *J. Phys. Chem. B*, 2007, **111**, 11817; Y. Hong, M. Ha¨ubler, J. W. Y. Lam, Z. Li, K. K. Sin, Y. Dong, H. Tong, J. Liu, A. Qin, R. Renneberg and B. Z. Tang, *Chem. Eur. J*., 2008, **14**, 6428; M. Wang, X. Gu, G. Zhang, D. Zhang and D. Zhu, *Anal. Chem.*, 2009, **81**, 4444; Q. Chen, N. Bian, C. Cao, X.-L. Qiu, A.-D. Qi and B.-H. Han, *Chem. Commun.*, 2010, **46**, 4067; T. Sanji, K. Shiraishi, M. Nakamura and M. Tanaka, *Chem. Asian J*., 2010, **5**, 817.

8 H. Shi, R. T. K. Kwok, J. Liu, B. Xing, B. Z. Tang and B. Liu, *J. Am. Chem. Soc.*, 2012, **134**, 17972.

9 L. Liu, G. Zhang, J. Xiang, D. Zhang and D. Zhu, *Org. Lett.*, 2008, **10**, 4581.

10 P. P. Kapadia, J. C. Widen, M. A. Magnus, D. C. Swenson and F. C. Pigge, *Tetrahedron Lett*., 2011, **52**, 2519.

11 Y.-R. Zheng, Z. Zhao, M. Wang, K. Ghosh, J. B. Pollock, T. R. Cook and P. J. Stang, *J. Am. Chem. Soc*., 2010, **132**, 16873; G. Huang, G. Zhang and D. Zhang, *Chem. Commun.*, 2012, **48**, 7504.

12 G. Huang, G. Zhang and D. Zhang *Chem. Commun*., 2012, **48**, 7504.

13 F. C. Pigge, P. P. Kapadia and D. C. Swenson, *CrystEngComm*, 2013, **15**, 4386.

14 S. V. Bhosale, M. Adsul, G.V. Shitre, S. R. Bobe, S. V. Bhosale and Steven H. Privér, *Chem. Eur. J*., 2013, **19**, 7310.

15 D. Ke, C. Zhan, S. Xu, X. Ding, A. Peng, J. Sun, S. He, A. D. Q. Li, J. Yao, J. Am. Chem. Soc. 2011, 133, 11022.

16 C. Röger and F. Würthner, *J. Org. Chem.*, 2007, **72**, 8070.

17 F. Miao, G. Song, Y. Sun, Y. Liu, F. Guo, W. Zhang, M. Tian, X. Yu, *Biosensors and Bioelectronics*, 2013, **50**, 42.

18 M. J. Frisch *et al*., Gaussian 09, revision D.01, *Gaussian*, Inc., Wallingford CT (2013).

19 W. Qunyan, D. Chunmei, P. Qian; N. Yingli, S. Zhigang *J. Comp. Chem.*, 2012, **33**, 1862.

20 S. Ghosh, X. Q. Li, V. Stepanenko, F. Würthner, *Chem. Eur. J*., 2008, **14**, 11343.

21 R. Davis, N. S. S. Kumar, S. Abraham, C. H. Suresh, N. P. Rath, N. Tamaoki and S. Das, *J. Phys. Chem. C*, 2008, **112**, 2137.

Graphical Abstract

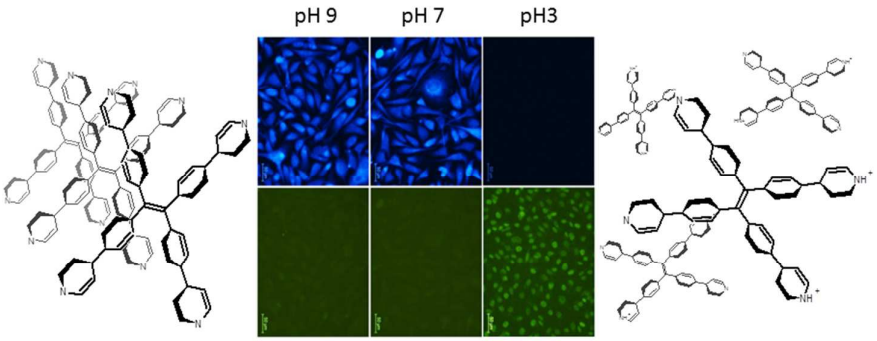

A pyridyl functionalised tetraphenylethylene (Py-TPE) for ratiometric fluorescent for precise aggregation-induced emission enhancement *via* H^+ sensing and its use in ratiometric detection of intracellular pH values is reported.